International Journal of Engineering Research
Volume No.9, Issue No.1, pp: 10-16
ISSN: 2319-6890 (online),2347-5013(print)
1 Jan. 2020

External Magnetic Field and Air mass Effects on Electrical Parameters of a Bifacial Solar Cell under Transient State

Alain Diasso[1], Raguilignaba Sam[1,2]; and François Zougmoré[1]
[1]Laboratoire de Matériaux et Environnement, UFR/ST, Université de Ouagadougou, 03 BP 7021 Ouagadougou, Burkina Faso.
[2]Departement de physique, UFR/ST, Université Polytechnique de Bobo-Dioulasso, 01 BP 1091 Bobo 01, Burkina Faso.
Corresponding Email:alinodiass@yahoo.fr

***Abstract:** This manuscript presents external magnetic field and air mass effects on electrical parameters in polycrystalline silicon solar cell under a multispectral flash illumination. Firstly, from a theoretical approach based on the columnar model of the grains and the quasi-neutral base, the three-dimensional diffusion equation is established. Also the boundaries conditions are defined in order to use Green's functions to solve this equation. Secondly, magnetic field and air mass effects on carriers' density and transient voltage are presented. Thirdly,magnetic field and air mass effects are pointed out on electrical parameters such as shunt and series resistances and junction capacitance.*

Keywords: Air mass; Junction capacitance; Magnetic field, Series and shunt resistances

1. Introduction

In order to reduce dependence on fossil fuels, renewable energy sources have been studied intensively for many years [1]. As solar energy, one major source of renewable energies, depends on the fluctuating solar radiation and solar cell properties.

However, solar spectrum and fields are environmental factors that affects the performance of solar cell. Air mass and magnetic field are two of the factors that influences respectively the solar spectrum and solar cell efficiency [2-3].Nowadays a lot of solar cells research high performance or solar cells operating under conditions that reduce solar cells performances factors limiting: minority carrier recombination photogenerated in the basis [4], in surface and grains boundaries [5], photocurrent and photovoltage losses, shadiness effects and resistive losses [6].The electronic and electrical parameters of the solar cell are closely dependent on carrier distribution in the solar cell. The magnetic field and the air mass affected these parameters [7-8-9].

2. Method and material

In this study based on a 3D modeling of a polycrystalline silicon solar cell; we made the following hypothesis:

- Considering the weak thickness of the emitter and zone of space load, we neglected their contributions to the photocurrent, so the quasi-totality of the current is provided therefore by the base [6; 7].

- The grains are under shape parallelepipedic (2a; 2b; H) and the joints of grains are perpendicular to the junction;

-The surfaces between two adjacent grains and perpendicular to the junction are characterized by the same carrier recombination processes evaluated by a grain boundary recombination velocity $Sgx = Sgy = Sg$;

- The electric field of crystal lattice is negligible [10];

- Only the contribution of the base in the processes of generation is considered; the magnetic field is oriented according to the direction $\overrightarrow{oy}$, $\vec{B} = B\overrightarrow{oy}$ .It is therefore perpendicular to the depth of light penetration in order to observe the effect of the strength of Lorentzon the carriers;

-The illumination is uniform. Then we have a generation rate depending only on the depth in the base z;

-The solar cell is front side illuminated under the external magnetic field and the tree type of air mass is illustrated on figure 1 [11].

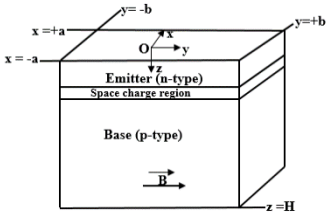

Figure 1: A model of grain in the polycrystalline sample.

In the base of the cell, the minority carriers are electrons, and their density satisfies to the equation below:

$$\frac{\partial \delta n}{\partial t} = \frac{1}{e}\vec{\nabla}.\vec{j}_n + g_n - r_n \qquad (1)$$

g_n, r_n are respectively the rate of generation and recombination of carriers. The current density $\vec{j}_n$ is given by:

$$\vec{j}_n = eD_n\vec{\nabla}\delta_n + e\mu_n\vec{E} - \mu_n\vec{j}_n\Lambda\vec{B} \qquad (2)$$

ISSN: 2319-6890 (online),2347-5013(print)
1 Jan. 2020

$\vec{E}$ is the electric field of the crystal lattice and μ_n is the mobility of the electrons.

Substituting equation (2) into (1) and taking into account the assumption of quasi-neutrality of the base, the diffusion equation of the electrons in the base becomes the equation 3:

$$\frac{\partial \delta(x,y,z,t)}{\partial t} - D^* \left(\vec{\nabla}\delta(x,y,z,t) - \frac{\delta(x,y,z,t)}{L^*} \right) = g(x,y,z,t)$$

$$\theta = 1 + (\mu B)^2 \quad (4)$$

D^* is the diffusion coefficient of excess minority carriers in the base of the bifacial cell in presence of magnetic field [12;13]; it can be expressed as:

$$D^* = \frac{D}{1 + (\mu B)^2} \quad (5)$$

D , μ , B are respectively coefficient of electrons diffusion, mobility of electrons and the value of magnetic field applied.

The presence of the magnetic field in our model lead to new values of carrier diffusion length L^* and carrier diffusion coefficient D^* which depend on magnetic field. θ is a coefficient which depend on magnetic field intensity.The carriers' generation rate under multispectral light at the depth z in the base can be written by the following expression:

$$g(z,t) = \begin{cases} n.\sum_{n=1}^{3} a_m \exp(-b_m z) & \text{si } 0 \le t \le Te \\ 0 & \text{si } t \succ Te \end{cases} \quad (6)$$

In this expression of $g(z,t)$, $n = \frac{I_{cci}}{I_{cco}}$ indicates the illumination level. The coefficients a_m and b_m are the modeling coefficients of AM1.5, AM1 and AM0 of air mass [14; 15].

Equation (1) is solved with the following boundary conditions:

- At the junction z = 0

$$\left.\frac{\partial \delta(x,y,z,t)}{\partial z}\right|_{z=0} = \frac{Sf}{D^*}\delta(x,y,z=0,t) \quad (7)$$

- At the rear side z = H

$$\left.\frac{\partial \delta(x,y,z,t)}{\partial z}\right|_{z=H} = \frac{Sb}{D^*}\delta(x,y,z=H,t) \quad (8)$$

- At surfaces limited by $x = \pm a$ and $y = \pm b$

$$\left.\frac{\partial \delta(x,y,z,t)}{\partial x}\right|_{x=\pm a} = \pm\frac{Sgx}{D^*}\delta(x=\pm a,y,z,t) \quad (9)$$

$$\left.\frac{\partial \delta(x,y,z,t)}{\partial y}\right|_{y=\pm b} = \pm\frac{Sgy}{D^*}\delta(x,y=\pm b,z,t) \quad (10)$$

Sf , Sb and Sg are the recombination velocity of minority carriers respectively at surfaces $z = 0$, $z = H$ and $x = \pm a$ (or $y = \pm b$).

a, b and H are the grain sizes as indicated on figure 1.

A solution of equation (1) is given by expression (11) according to the author of the reference [11].

$$G = \sum_{i=1}^{+\infty}\sum_{j=1}^{+\infty}\sum_{k=1}^{+\infty} M_i M_j M_k \exp\left(-\beta\left(t - t'\right)\right)$$

(11)

where:

$$M_i = A^2_{k_i}\cos(k_i x')\cos(k_i x) \quad (12)$$

$$M_j = A^2_{l_j}\cos(l^*_j y')\cos(l^*_j y) \quad (13)$$

$$M_k = A^2_{\mu_k}\cos(\mu_k z' + \varphi_k)\cos(\mu_k z + \varphi_k) \quad (14)$$

β^* and l^*_j are expressed by:

$$\beta^* = D^*\left(k^2_i + l^2_j + \mu^2_k + \frac{1}{L^{*2}}\right) \quad (15)$$

$$l^*_j = \frac{l_j}{\sqrt{\theta}} \quad (16)$$

The expression (11) can write simply by the following equation:

$$\delta_1(x,y,z = \left[\frac{4.n.a_m.A^2_{k_{i,1}}.A^2_{l_{j,1}}.A^2_{\mu_{k,1}}\sin(k_{i,1}a)\sin(\frac{l_{j,1}}{\sqrt{\theta}}b)}{k_{i,1}\frac{l_{j,1}}{\sqrt{\theta}}\beta^*}K \times \cos(k_{i,1}.x).\cos(\frac{l_{j,1}}{\sqrt{\theta}}y)\cos(\mu_{k,1}z + \varphi_{k,1})\right].F_0(t)$$

is the expression of carriers density. Where:

$$F_0(t) = \left(1 - \exp(-\beta^* Te)\right).\exp(-\beta^*(t - Te)) \quad (18)$$

ISSN: 2319-6890 (online),2347-5013(print)
1 Jan. 2020

$$K = \frac{a_m.b_m}{b_m^{\ 2} + \mu_k^{\ 2}} \left[\begin{array}{l} -\exp(-b_m.H)\cos(\mu_k.H + \varphi_k) + \cos(\varphi_k) + \\ \frac{\mu_k}{b_m}\exp(b_m.H) \times \sin(\mu_k.H + \varphi_k) - \frac{\mu_k}{b_m}\sin(\varphi_k) \end{array} \right] \quad (19)$$

The quantities A_{l_i}, A_{l_j} and A_{μ_k} are obtained by normalizing M_i, M_j and M_k. The parameters k_i, l_j and μ_k are the eigen values obtained from the boundary conditions. φ_k is the initial phase and obtained by solving the equation

$$\tan(\mu_k H + \varphi_k) = \frac{Sb}{\mu_k D^*} \quad (20)$$

The transient voltage decay is defined by the next equation:

$$V(t) = V_T Fv\left(k_1; l^*_1; \mu_1\right) r \exp\left(-\beta(t - Te)\right) \quad (21)$$

where $r = \exp\left(\frac{\Delta V}{V_T}\right) - 1$ and $\Delta V = V_O - V_F$ (22)

$$Fv(k_1, l^*_1, \mu_1) = \frac{\Delta_0(0,0)}{\Delta(0,0)}.\left[1 - \exp\left(-\beta^*.Te\right)\right] \quad (23)$$

The quantities $\Delta_0(0,0)$ and $\Delta(0,0)$ are defined by:

$$\Delta_0(0,0) = \int_{-a}^{a}\int_{-b}^{b} Z_{111}(x,y,0)\,dxdy \quad (24)$$

$$\Delta(0,0) = \int_{-a}^{a}\int_{-b}^{b} d_{111}(x,y,0)\,dxdy \quad (25)$$

$Z_{111}(x,y,0)$ and $d_{111}(x,y,0)$ are respectively the spatial component of $\delta(x,y,z,t)$ and the minority carrier density during the phase of illumination.

$$l^*_1 = \frac{l_1}{\sqrt{\theta}} \quad (26)$$

According to expression (18), we notice two types of $V(t)$ decays:

- if $Fv\left(k_1; l^*_1; \mu_1\right) r \exp\left(-\beta^*(t - Te)\right) \prec\prec 1$

The time dependent tension is rewritten in the following way:

$$V(t) = V_T\left[-\beta^*(t - Te) + \ln\left(1 + Fv\left(k_1; l^*_1; \mu_1\right)\right) r\right] \quad (27)$$

This is a linear function of the time with a negative slope $-V_T\beta^*$

- if $Fv\left(k_1; l^*_1; \mu_1\right) r \exp\left(-\beta^*(t - Te)\right) \succ\succ 1$

$V(t)$ can be rewritten in the form :

$$V(t) = V_T Fv\left(k_1; l^*_1; \mu_1\right) r \exp\left(-\beta(t - Te)\right) \quad (28)$$

$V(t)$ is a time dependent decay exponential function.

3 .RESULTS AND DISCUSSION

We present here the simulation results obtained from the previous modeling equations.

3.1. Effects of magnetic field and air mass on carrier density

We presents here the curves of carriers' density versus air mass and magnetic field.

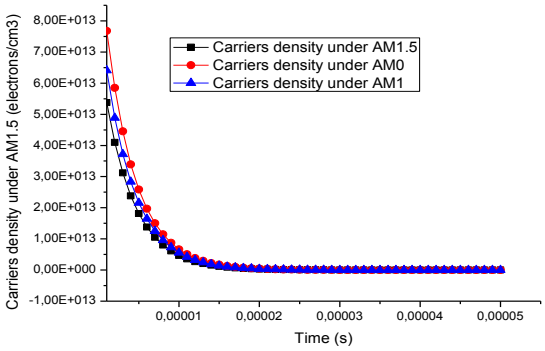

Figure 2: Carriers density curves versus air mass and time.

This decay can be explain by the reducing of the generation rate during the time to the different air mass. So when the air mass increase, the direction of normal irradiance decrease reducing carriers' generation.

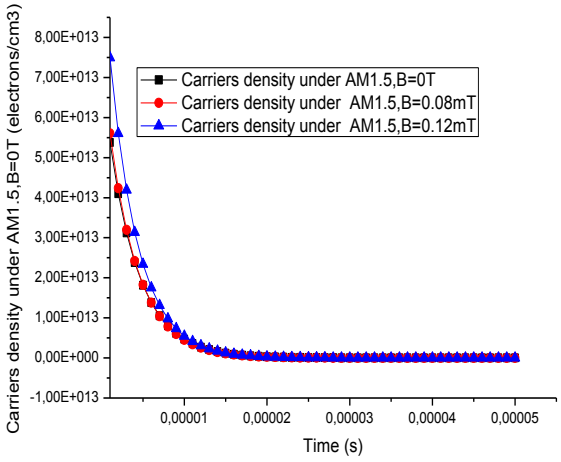

Figure 3: Carriers density curves versus magnetic field and time.

The figure 4 presents the variation of carriers' density versus magnetic field and time. The figure 4 show that for increasing magnetic field, the maximum of the excess minority carriers' density increase also and are shifted left to the junction. This increasing of the maximum of the excess minority carriers' density translate an increase of the carrier concentration.

3.2. Effects of magnetic field and air mass on transient voltage

Transient voltage curves versus magnetic field is presented

ISSN: 2319-6890 (online),2347-5013(print)
1 Jan. 2020

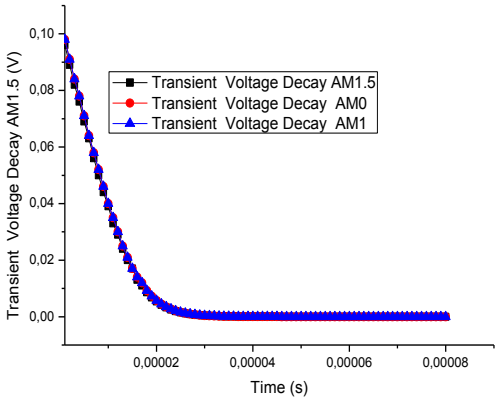

Figure 4: Transient voltage curve versus time for various air mass.

The figure 2 presents the curve of transient voltage decay with the air mass from air mass 0 to air mass 1.5 but we remark the same variation for air mass 0 and 1.This behavior is explain by the substantially identical values of air mass 0 and 1 .
The decrease of transient voltage to air mass 0 to air mass 1.5 is explain by an important photogeneration of excess minority carriers under AM0 than AM1.5.
The increasing of air mass creates the decrease of normal irradiance by reducing illumination then the number of excess minority carriers. In other words, much load carriers are stored near the junction under air mass 0 because much carriers are photogenerated.

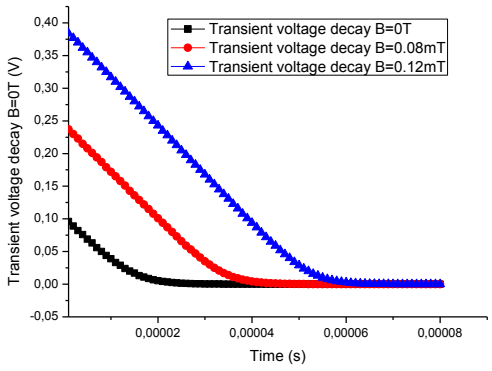

Figure 5: Transient voltage decay curves versus magnetic field.

The profile of figure 3 presents the transient voltage increasing when the magnetic field increases.
The transient voltage which means an accumulation of charges across the junction presents a maximum for very low S_f values (open circuit); this open circuit voltage increases with increasing magnetic field. This is a consequence of charge accumulation in the base and diminution of junction recombination with increasing magnetic field; this phenomenon is accompanied by an increase of recombination in the bulk and at the grain boundaries [13; 16].
The behavior of the transient voltage under magnetic field characterizes an increase of resistive losses in the base (due to material structure and electrical grids); this increase of resistive losses leads to a decrease in the output voltage.
From our previous results, we propose below an equivalent electrical model for the solar cell under external magnetic field and air mass.

3.2. Equivalent electrical model of the solar cell under magnetic field and different air mass

We present on figure 4 the equivalent electrical one diode model of the solar cell under magnetic field and different air mass:

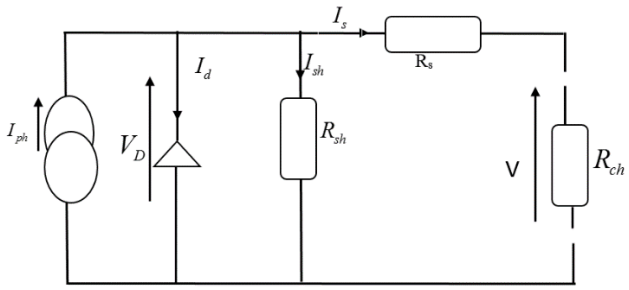

Figure 6: Equivalent electrical model of the solar cell under magnetic field and different air mass.

In this model, the diode characterizes not only the diffusion saturation current in the base and the emitter but also the generation-recombination saturation current in the space charge region [4-10]. It appears also in this model two parasitic resistances [5].The shunt resistance R_{sh} characterizes currentlosses at the junction. These losses are induced byintrinsic recombination (Sf_0) at the junction. Then a partof the photocurrent is derived from this resistance andcould not be used by the external load.The series resistance R_s characterizes the contacts resistance, the resistivity of the base material and the dynamic resistance of the junction [6]. The presence of this resistance leads to a decrease of the voltage across the external load.It is a fundamental parameter [18] depending on the semiconductor substrate, the temperature and the fabrication technology.

3.3. Effects of magnetic field and air mass on junction capacitance

To exhibit the capacitive effects of the space charge region;we introduce the capacitor with capacitance C to the place of the diode.The solar cell junction behaves like a capacitor with capacitance [6; 19] depending on the space charge region width. So the equivalent model become 7:

ISSN: 2319-6890 (online),2347-5013(print)
1 Jan. 2020

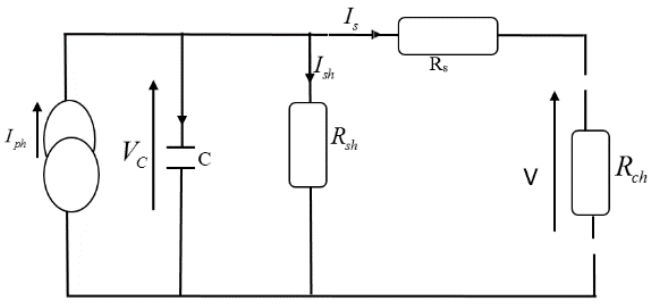

Figure 7: Equivalent electrical model of solar cell

Based on the carrier density in the base, the junction under magnetic field capacitance is given by [20].

$$C(a_n, b_n, B) = \frac{Q(a_n, b_n, B)}{V(a_n, b_n, B)} \quad (29)$$

with the following equation :

$$Q(a_n, b_n, B) = q \int_{-a}^{a} \int_{-b}^{b} \delta(x, y, 0, a_n, b_n, B)\, dx\, dy \quad (30)$$

where: -q: is the elementary charge. -V: is the transient voltage across the junction.

We present here the junction capacitance with magnetic field for various air mass.

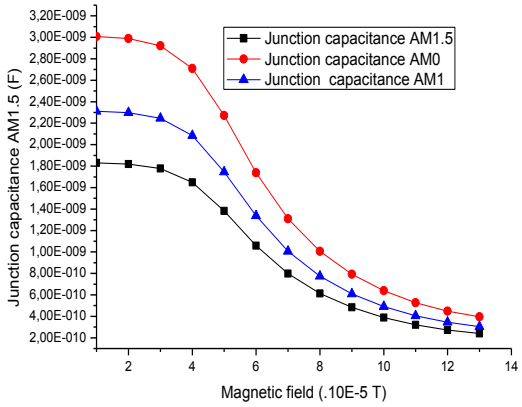

Figure 8: Capacitance decay curve versus magnetic field for various air mass

The curves of figure 8 shows the decay of junction capacitance with the magnetic field.

The junction capacitance seems not to depend on magnetic field for values less than $B = 4.10^{-5} T$. But for more intense magnetic field, the junction capacitance decreases very rapidly.

This behavior of the junction capacitance is directly related to the space charge region widening with magnetic field.

Indeed, the junction capacitance depends on the charge of carriers, it is well understandable that the junction capacitance is great under AM0, than AM1 or AM1.5 because the concentration of carrier in the base is then decrease from AM0 to AM1.5 so that the capacitance also decreased in this way. Also the generation rate can explain this behavior of junction capacity because the values of generation rate is great under AM0 than others.

3.4. Effects of magnetic field and air mass on series resistance

Near open circuit, the solar cell operate like a real voltage generator, that is an association of an ideal voltage generator and an internal series resistance R_s which causes a voltage drop and thus decreasing the output voltage. The determination of this series resistance is made near the open circuit. Near this operating point there is a charge accumulation in the cell so that any loss is due to the cell structure and electrical grids.

Near this open circuit, the solar cell can be represented by the following electrical model [12; 18; 21; 22]

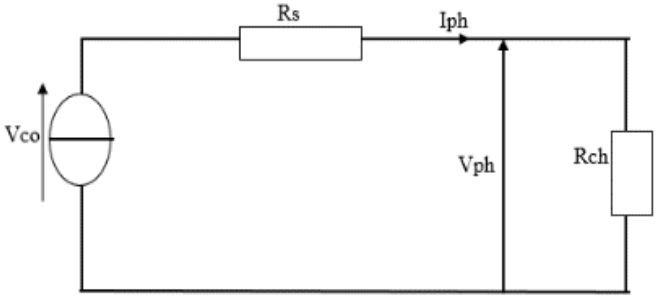

Figure 9: Electrical model of the solar cell near open circuit.

The load resistance R_{ch} is taken very low to keep the solar cell close to the short circuit. The expression of series resistance giving by the following mathematical relation:

$$R_s(a_n; b_n; B) = \frac{V_{oc}(a_n; b_n; B) - V_{ph}(a_n; b_n; B)}{I_{ph}(a_n; b_n; B)} \quad (31)$$

The curve of figure 10 present the influences of the magnetic field and air mass on series resistance.

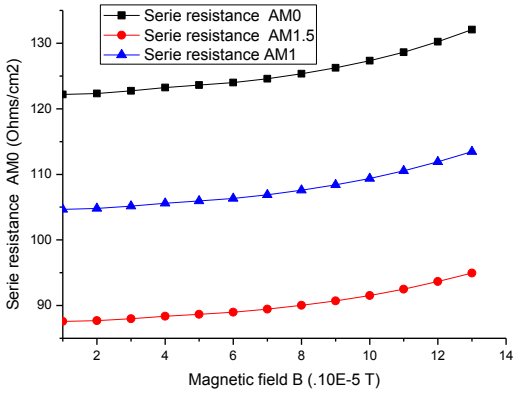

Figure 10: Series resistance curve versus magnetic field for various air mass.

ISSN: 2319-6890 (online),2347-5013(print)
1 Jan. 2020

It can be notified that the series resistance increase with the magnetic field called magneto resistance [6]. As noted of junction capacitance; the series resistance for the values of magnetic field $B \leq 4.10^{-5}T$, increase slowly but more marked for $B \succ 4.10^{-5}T$. So when the magnetic field increases, the diffusion coefficient decreases considerably because of the incurved path of carriers due to Lorentz law.
Also; the magnetic created the braking of carriers decreasing the loss of load carriers.
Indeed, relatively to the air mass to AM1.5 to AM0, the series resistance increase. This is the consequences of the carrier's density which is greater than other air mass hoverer the loss that the load carriers can be suffered. So AM0 optimize series resistance operating.

3.5. Effects of magnetic field and air mass on shunt resistance

The shunt resistance R_{sh} [6] results from carrier recombination in the bulk and the interfaces of the cell. R_{sh} characterizes the leakage current in the cell; the higher R_{sh} is, the lower the leakage current is considering the solar cell near short circuit, the behavior of current generator lead us to represent the system solar cell+load‖ as follow (figure 11) [12;18;21;22]:

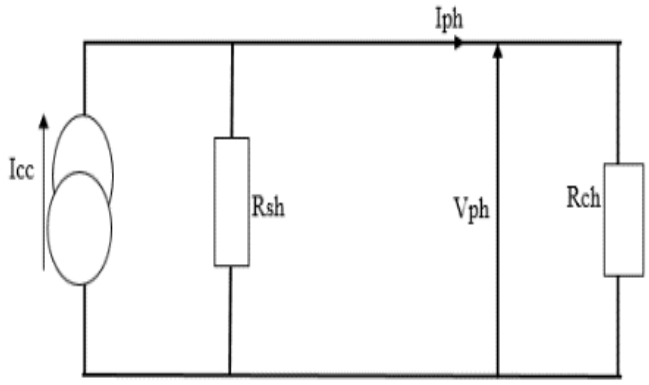

Figure 11: Equivalent electrical model of the solar cell in short circuit

Shunt resistance expression is given by:

$$R_{sh}(a_n;b_n;B) = \frac{V_{ph}(a_n;b_n;B)}{I_{cc}(a_n;b_n;B) - I_{ph}(a_n;b_n;B)}$$

(32)

We present the effects of magnetic field and air mass on this figure

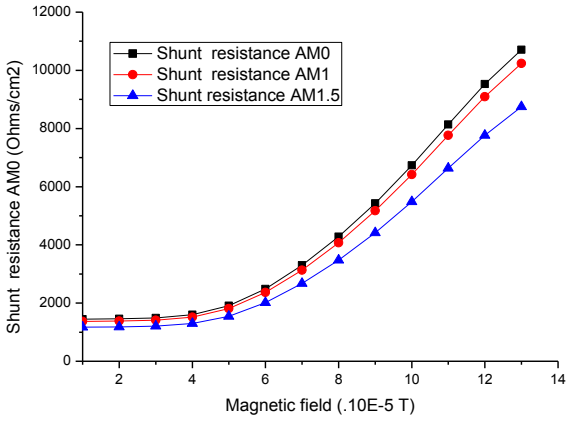

Figure 12: Shunt resistance curve versus magnetic field for various air mass.

The profile of curves of shunt resistance with the magnetic field and air mass show that, the shunt resistance increases slowly for the small values of magnetic field $B \leq 4.10^{-5}T$ and rapidly for the values of magnetic field $B \geq 4.10^{-5}T$.
Shunt resistance also increase with magnetic field; when magnetic field increases, the number of excess minority carrier crossing the junction will decrease because essentially of incurvated path, that is, the leakage current of the junction will also decrease and this decrease correspond to an increase of the shunt resistance.

Comparatively to the magnetic field; the shunt resistance decrease with the air mass from air mass 0 to air mass 1.5 however the loss of load carriers in grains boundaries or to the junction; the width of light spectrum AM.5 have the greater loss than AM1 and AM0.Then the loss of load carriers or the recombination are not sensitive with the AM0 than AM1 and AM1.5.

It was shown that magnetic field decreases junction capacitance and increase series and shunt resistances.

4. CONCLUSION

This 3D study of magnetic field effect and air mass on solar cell lead us to put in evidence analytical expressions of carriers density and transient voltage in the base of the solar cell and electrical parameters such as; R_s; R_{sh} *and* C .It was shown that magnetic field decreases junction capacitance and increase series and shunt resistances. It seems that magnetic field less than $4.10^{-5}T$ has no effect on electrical parameters

The analysis of the magnetic field and air mass effects show practically that terrestrial magnetic field and electromagnetic waves (AM antenna and FM antenna) has not effects on solar cell.

Globally the magnetic field has negative effects and AM0 was the air mass which optimizes solar cell operating.

References

i. *Ellabban O and al. Renewable energy resources: Current status, future prospects and their enabling technology. Renewable and SustainableEnergyReviews 2014; 39: 748–764.*

ii. *Khalid S Rida and al;The impact of air mass on photovoltaic panel performance; doi:10.18282/ser.v1.i1.41;disco med publishing*

iii. *S. Madougou and al: I –V Characteristics For Bifacial Silicon Solar Cell Studied Under a Magnetic Field; Advanced Materials Research Vols. 18-19 (August 2007) pp. 303-312*

iv. *B. Equer : Energie solaire photovoltaïque, volume 1,1993, Ellipses.*

v. *A. Rocher :''Origine structurale et chimique de l'activité des joints de grain dans le silicium'' Revue de Physique Appliqué, 22, (1987), 591-595.*

vi. *J.P Charles and al : ''La Jonction du Solaire à la Microélectronique'' Rev. Energ. Ren. , 3; 2000, 1-16*

vii. *F. Toure and al: Influence of Magnetic Field on Electrical Model and Electrical Parameters of a Solar Cell under Intense Multispectral Illumination, Global Journal of Science Frontier Research Physics and Space Sciences Volume 12 Issue 6 Version 1.0 Year 2012.*

viii. *IssaZerbo and al: External Magnetic Field Effect on BifacialSilicon Solar Cell's Electrical Parameters, Energy and Power Engineering, 2016, 8, 146-151*

ix. *A.D. Pene and al: Influence of Magnetic Field on the Electrical Parameter of A Bifacial Silicon Solar Cell Front Side Illuminated by A Multispectral Light Under Steady State;International Journal of Emerging Technology and Advanced Engineering*

x. *R Sam and al:3D determination of the minority carrier lifetime and the p-n junction recombination velocity of a polycrystalline silicon solar cell; 1st International Symposium on Electrical Arc and Thermal Plasmas in Africa (ISAPA); doi:10.1088/1757-899X/29/1/012018*

xi. *R. Sam and al :A Three-Dimensional Transient Study of a Polycrystalline Silicon Solar Cell under Constant Magnetic Field;];International Journal of Engineering Research Volume No.5, Issue No.2, pp.: 93- 97*

xii. *Th. Flohr and R. Helbig, Determination of minority carrier lifetime and surface recombination velocity by Optical-Beam-Induced- Current measurements at different light wavelengths, J. Appl. Phys. Vol.66 (7), (1989) pp 3060 – 3065.*

xiii. *A. Dieng and al: Magnetic Field Effect on the Electrical Parameters of a Polycrystalline Silicon Solar Cell; Research Journal of Applied Science, Engineering and Technology 3(7): 602-611, 2011*

xiv. *Joze et al: Approximation of the carrier generation rate in illuminated silicon; Solid State Electronics vol 28; No 12; pp. 1241-1243.1985*

xv. *S.N. Mohammad; An alternative method for the performance analysis of silicon solar cells, J. Appl. Phys. 61 (2), (1987) pp 767 – 777*

xvi. *M. Zoungrana and al: 3D Study of Bifacial Silicon Solar Cell Under Intense Light Concentration ExternalConstantMagnetic Field: Effect Of Magnetic Field And Base Depth On Excess Minority Carrier Generation.*

xvii. *J.M Asensi and al:"Shortcircuit resistance a-Si:HP-I-N solar cells: the link with the electronic properties of the active layer", Proc.2nd World conference and exhibition on photovoltaic solar energy conversion ,1, 1998, 906-909.*

xviii. *S. Mbodji and al: Modeling Study of N+/P Solar Cell Resistances from Single I-V Characteristic Curve Considering the Junction Recombination Velocity (Sf) Re-search Journal of Applied Sciences, Engineering and Technology 4(1): 1-7, 2012*

xix. *N.V Philips:''Practical electronics'', gloeilampenfabrieken, 1966*

xx. *G. Sissoko and al:Silicon solar cell space charge width determination by study in modelling ", Proc. World Renewable Energy Congress,1998, 1852-1855.*

xxi. *M.L.Samb and al :Etude en modélisation à 3-D d'une photopile au silicium en régime statique sous éclairement multispectrale : détermination des paramètres électriques", J. Sci.Vol. 9, N° 4 (2009) 36 – 50; http ://www.cadjds.org*

xxii. *A. Dieng and al :A Bifacial Silicon Solar Cell Parameters Determination by Impedance Spectroscopy", Proceedings of the 22nd European Photovoltaic Solar Energy Conference and Exhibition (2007), pp.436-440*